JOURNAL OF OPTOELECTRONICS AND ADVANCED MATERIALS Vol. 16, No. 3-4, March - April 2014, p. 243- 251

Avalanche breakdown in amorphous selenium (a-Se) and related materials: Brief review, critique, and proposal

K. TANAKA*
Department of Applied Physics, Graduate School of Engineering, Hokkaido University, Sapporo Kita-ku, 060-8628, Japan

Optically-triggered avalanche breakdown in a-Se films has been amply demonstrated and analyzed recently on the basis of a lucky-drift model, while the analyses seem to pose perplexing problems. We suggest a new idea, which takes disordered structures in a-Se into account with an assumption of two kinds of impact ionization processes. This model provides plausible parameters for the avalanche behavior and reasonable explanations for temperature dependence. We also discuss similar phenomena in other amorphous materials.

(Received January 15, 2014; accepted March 13, 2014)

Keywords: Avalanche, Amorphous, Selenium, High field, Transport

1. Introduction

In a long research history of the electric breakdown in solids after 1930's [1], one of the epoch-making may be the discovery of *impact avalanche breakdown in a disordered semiconductor*, a-Se, by Juška and Arlauskas [2,3]. Moreover, Tanioka et al. [4] demonstrated photocurrent multiplication in electron-beam scanned a-Se targets, the phenomenon being already commercialized as HARP (high-gain avalanche rushing photoconductor) vidicons [5,6] and further developed to flat imaging devices [7], x-ray detectors [8-11], and Se/As_2Se_3 multi-layer photodiodes [12]. On the other hand, fundamental avalanche characteristics have experimentally been investigated [13-18], and the results have theoretically been analyzed [19-25] using impact-ionization models originally proposed for crystalline semiconductors [8,26-31]. A recent model has been applied also to interpretations of high-field photoconduction in a-Si:H and electrical switching (giving rise to high-conducting states and ultimately thermal phase changes from amorphous to crystalline) in a-$Ge_2Sb_2Te_5$ [15,21,22,24].

However, the analyses appear to be confronted with difficult problems, as described later, which should be shed light from bird's-eye views. In addition, the studies on a-Se have been conducted mostly in limited groups in former USSR [2,3], Japan [4,5,7,9,12-14], and Canada [10,11,15-25]. Hence, further interests from wider perspectives will be valuable for understanding the breakdown mechanism in disordered semiconductors.

In the present work, we briefly review research history of the avalanche breakdown in a-Se (Sections 2 and 3) with some comments (Section 4), and propose a new idea for the breakdown mechanism (Section 5). The approach adopted herein is heuristic and tentative, but important results are explainable without complicated calculations. We also discuss (Section 6) differences between the breakdown in a-Se and similar phenomena in other inorganic [32-39] and organic materials [40-43].

2. Observations

Table 1 summarizes experimental conditions employed for investigating high-field phenomena in a-Se films. Experiments have been performed using four different arrangements, which are fixed in combinations of two kinds of sample structures and light excitations. The structure is either of sandwiched (stacked) electrodes or a vidicon type (HARP). In both structures, carrier injection is suppressed using insulating polymer layers (PET) or some inorganic films (CeO_2, Sb_2S_3) having appropriate work functions. Light excitations are supplied as pulses in optical time-of-flight (TOF) experiments, which can evaluate carrier mobility, or as continuous waves (cw) for spectral and other measurements. Note that, among all the experimental results, Tsujis' [14] covers up to the highest field of 1.6 MV/cm (Fig. 1(b) and Fig. 2), which could be attained using thin a-Se films of 0.5 μm; this thickness is still much greater than the penetration depth (~0.03 μm) of light, which varies at 0.03 − 1 μm with light wavelengths of 400 – 600 nm at room temperature [44], and accordingly, a sufficiently thick region (~0.47 μm) remains for avalanche multiplication of carriers.

Table 1. Summary of experimental (Sample structure − T) and theoretical ($L_{elastic}$ − E_i) studies on the avalanche breakdown in a-Se, listed in a historical order. F denotes the electric field, T the sample temperature, $L_{elastic}$ and L the mean free-paths of holes determined by elastic and inelastic scatterings, E_R the vibrational (optical phonon) energy, E_i the impact-ionization energy, RT room temperature, and x unrelated. In the sample structure, M represents a metal film, PET a thin polyethylene-terephthalate layer, ITO a transparent In-Sn-O film, CA a resistive layer of spin-coated cellulose acetate, and p and n signify positive and negative electrodes. HARP has a structure of p/ITO/CeO_2/a-Se/Sb_2S_3, on which light is incident from the left-hand side and the Sb_2S_3 back surface is scanned by an electron beam in vacuum. In experiments of Tsuji et al. [14] and Bubon et al. [17], light beams impinge on the asymmetric samples from the left- and right-hand sides for exciting hole and electron flows, respectively.
Theoretical parameters for Tsuji are determined in the present work using Eq. (1).

Reference	Sample structure (with film thicknesses in μm)	Method	Light	F (MV /cm)	T (K)	$L_{elastic}$ (nm)	L (nm)	E_R (meV)	E_i (eV)
Juška [3]	M/PET/a-Se(3−200)/PET/M	TOF	N_2 laser	≤ 1	170 - 300	x	2.7	x	2.4
Tsuji [14]	p/Al/CeO_2/a-Se(0.5−4)/Au /n	cw	400 - 600 nm	≤ 1.6	100 - 300	x	0.6	x	0.56 (~1 MV/cm)
							2.6	x	1.9 (~1.4 MV/cm)
Arhipov [19]						x	0.6	x	0.55
Rubel [20]						0.6	3.6	40	0.8
Kasap [21]						0.3	4−6	x	1 or 2
Reznik [15]	M/PET/a-Se(4−33)/PET/M	TOF	blue light	< 1.1	RT	0.6	7.2	31	2.3
	HARP a-Se(8−35)	cw							
Reznik [16]	HARP a-Se(8−35)	cw	420 nm	<1.1	RT				
		TOF	337 nm		RT				
Jandieri[22]						0.3	2.4	31	2.3
Rubel [25]						0.5	4.3	31	2.3
Bubon [17]	p/ITO/CeO_2(0.01)/a-Se(15)/ Sb_2S_3(0.5)/CA(1)/Au/n	TOF	420 nm	≤ 1.04					
Reznik [18]	HARP a-Se(8)	cw	430 - 600 nm	≤ 1.13					

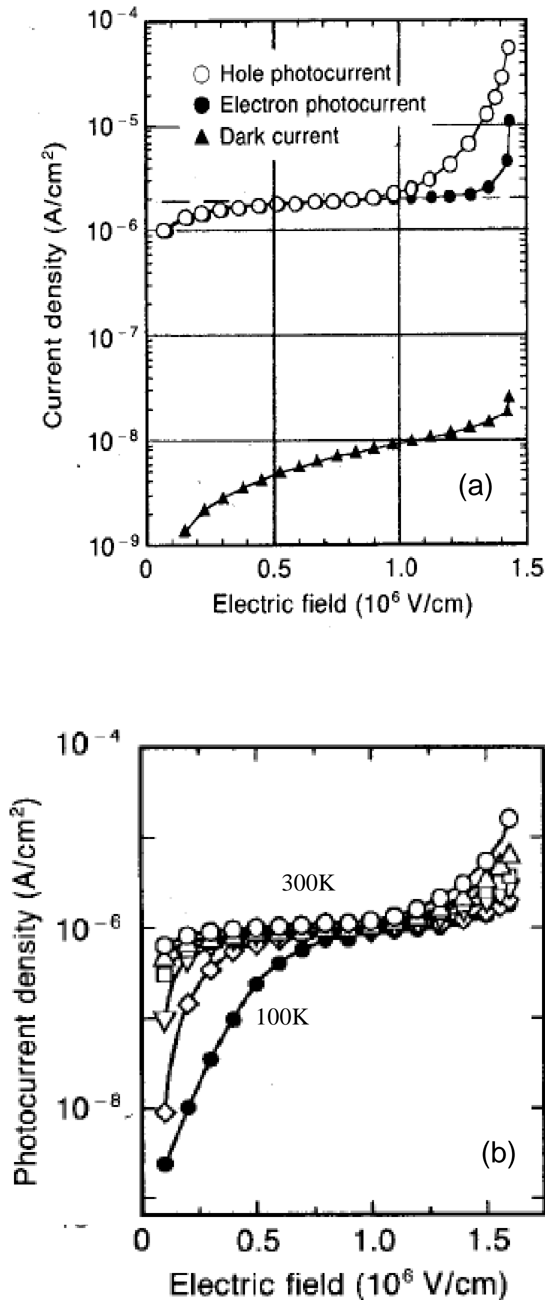

Fig. 1. Current densities in a-Se films with thicknesses of (a) 1 μm for hole and electron, and in a dark state at 5 s after switching off illumination, and of (b) 0.5 μm for hole as a function of temperature from 100 (●) to 120, 150, 170, 220, and 300 (○) K (modified from [14]).

Fig. 1 duplicates typical breakdown behaviors [14]. As shown in Fig. 1(a), holes are more efficiently multiplied than electrons, which is consistent with higher mobility of holes in a-Se [2,3,6,44]. The threshold fields F_t of hole and electron breakdowns are ~0.8 MV/cm and ~1.2 MV/cm at room temperature, which tend to decrease in thicker films [3,14]. Fig. 1(a) also shows that under the avalanche breakdown the current density J increases up to two orders of magnitude [2-5,13-17].

Here, an important parameter characterizing the avalanche multiplication is the impact-ionization rate (coefficient) γ. Experiments have demonstrated that J exponentially increases with the sample thickness d as $J \sim \exp(\gamma d)$, where γ is demonstrated to be independent of the film thickness ranging at $0.5 \leq d \leq 200$ μm [2,3,13,14,23]. Such a thickness dependence of J ($= en\mu$) is governed by an increase in the hole density n with a form of $n \sim \exp(\gamma x)$, where x ($= \mu F t$) is the distance of hole flows along the direction of an applied field F. On the other hand, the hole mobility μ is known to increase with increasing F toward ~1 cm^2/Vs [2,3,17].

As exemplified in Fig. 2 [25], all the results reported so far for $\gamma(F)$ are more-or-less quantitatively reproducible. However, since the sample structures are not simple (Table 1), including some insulators and doped (stabilized) regions [4], and in addition, photoconduction tends to modify the field distribution along a sample thickness, unavoidable errors may creep in the electric field F, which is evaluated from an applied voltage and a film thickness with some corrections [2,3]. Or, in HARP experiments, the electric field is estimated under an assumption that the voltage applied to un-illuminated (back) surfaces of a-Se targets is equal to an electron-gun voltage [4], which may add small errors.

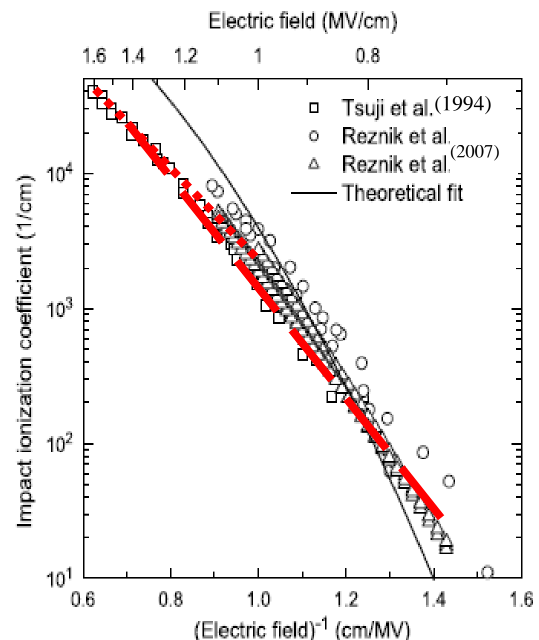

Fig. 2. Impact-ionization coefficients as a function of the electric field for holes in a-Se at room temperature (reproduced from [25] and modified with permissions). The solid line was calculated by Rubel et al. [25] using a modified lucky-drift model, and the dotted and dashed straight (red) lines delineate, respectively, the high- and low-field functions given by Tsuji et al. [14].

Marked observations obtained through those experiments can be summarized as follows:

1) No traces of carrier injection from electrodes have been detected, which manifests that the avalanche breakdown is not a contact-induced effect but a bulk phenomenon. Also, the fact that pulsed and cw excitations provide comparable results [15,21] negates thermal effects arising from Joule heating.

2) The avalanche breakdown is triggered by photogenerated carriers, specifically, holes. (After termination of light excitation, residual decaying currents reflecting slow electron motions flow [2,14,17], as shown in Fig. 1(a).) Nevertheless, photoconductive spectra [14,18] strongly suggest that the phenomenon so-called light impact-ionization [26,45,46] does not occur. In detail, the spectra reported [14,18] present some quantitative differences, the reason being not discussed. As known, in crystalline semiconductors with bulk forms or p-n junctions, the avalanche breakdown is brought by photo-, thermal, or injected carriers [26,30,31,47].

3) As shown in Fig. 1(b), carrier multiplication has been detected at temperatures of 100 − 300K with clear temperature-activated behaviors, i.e., $\partial\gamma/\partial T > 0$ and $\partial F_t/\partial T < 0$ [13,14]. The former possesses an activation energy of ~30 meV, which may decrease at higher fields. Note that the positive temperature dependence of γ is similar and *opposite* to those in Zener and avalanche breakdowns in crystalline semiconductors [1,8,48].

Incidentally, it is worth mentioning that the bulky avalanche breakdown is inherent only to the amorphous form of Se. Single crystalline Se samples subjected to high electric fields undergo piezoelectric acousto-electric current saturation, which suppresses the avalanche breakdown [44,49]. On the other hand, Kodeš [50] discovered prominent current rises in poly-crystalline Se rectifiers under high reverse voltages, yet the result seemed not to attract detailed experiments and analyses [44]. We may envisage a possibility that the current rise arises from Zener breakdown in polycrystalline junctions [51], which remains to be studied. It should also be mentioned here that, to the author's knowledge, there have been no reports of luminescence [26] from avalanching a-Se samples, while the spectrum may afford valuable insight.

3. Previous analyses

A central problem of the avalanche breakdown in a-Se is "Why can a field-induced impact ionization occur in a *disordered* semiconductor, in which carriers are far less mobile than those in crystalline semiconductors?". Actually, an ultimate microscopic hole mobility in a-Se appears to be, at most, ~1 cm^2/Vs [2,3,17], much smaller than those (~10^3 cm^2/Vs) in crystalline semiconductors, but despite of such a big difference, the threshold fields F_t in a-Se and c-AlGaAs (c- for crystalline), both having similar bandgap energies of ~2.0 eV, are comparable (~1 MV/cm and ~0.2 MV/cm [21]). Then, much effort has paid off for analyses of charge-multiplication behaviors, specifically $\gamma(F)$ (and F_t), which may be governed by the threshold energy E_i of impact ionizations that trigger the avalanche breakdown.

Pioneering researchers [2,3,19] have adopted a simple formula as;

$$\gamma = (1/L) \exp \{-E_i/(eFL)\}, \qquad (1)$$

where L is the carrier mean free path determined by inelastic scattering. This equation is based on the concept of a lucky-ballistic electron model, originally proposed by Shockley [26] for interpreting the breakdown in c-Si p-n junctions, which takes inelastic scattering with optical phonons and impact ionization into account. (His equation contains four parameters, path lengths and related energies for the two collision processes, some of which are difficult to evaluate.) However, it should be noted that the equation is derivable also from the lucky-drift model, described below, under a low-field limit [21,25,29].

As listed in Table 1, the early studies [3,14,19] gave E_i distributed over 0.5 − 2.4 eV, which is ascribable to different data and analyses employed. Juška and Arlaulas [2,3] derived their values through fitting Eq. (1) to their data. The Tsujis' result is calculated in the present work, as described later. In a theoretical work by Arkhipov and Kasap [19], moderate-field (~1 MV/cm) data of Tsujis' [13,14] were employed with Eq. (1), which gave the ionization energy of 0.55 eV for holes, substantially smaller than the optical gap E_g of ~2 eV in a-Se [44], which made them propose a *sub-gap* impact-ionization process. (Note that simplified assumptions provide $E_i \approx 1.5E_g$ in crystalline semiconductors [8,51].) They also interpreted the positive temperature dependence $\partial\gamma/\partial T > 0$ by assuming thermally-assisted dissociation of generated carrier pairs.

Afterwards, Rubel et al. [20] applied a lucky-drift model, proposed by Ridley [28], to the breakdown in a-Se, with reasoning that this model appeared more practical, and actually more successful, in describing the avalanche phenomenon in crystalline semiconductors. In the original formulation [28-31], a drifting carrier is assumed to undergo inelastic and also elastic scatterings, respectively, with optical and acoustic phonons. Rubel et al. [20] have modified the model so that in a-Se the elastic scattering is mediated also by disordered potentials. As listed in Table 1, analytical calculations [15] and Monte Carlo simulations [22,25] using such an idea, with a vibrational (optical phonon) energy E_R of ~30 meV, give $E_i \approx 2.3$ eV, which is similar to the bandgap energy. Also, the obtained parameters provide, e.g. γ(1 MV/cm) ≈ 1 ~ 10 μm^{-1} [15,21,23,25], in rough consistency with the observations (Fig. 2).

Theoretical studies have then been extended to two directions. One is the analyses of high-field behaviors in c-Se [53-55], which may provide deeper insights into the breakdown mechanism in a-Se. The other is the application of the modified lucky-drift model to other amorphous materials, a-Si:H [15,21] and a-$Ge_2Sb_2Te_5$ [22]. Reznik et al.

[15] compare breakdown characteristics in a-Se and a-Si:H ($E_g \approx 1.8$ eV), the latter exhibiting less steep current rises [33], and emphasize a role of higher phonon energy (~80 meV) in a-Si:H than that (~30 meV) in a-Se in energy dissipation processes of accelerated carriers. Jandieri et al. [22] apply the model to the electrical switching in a-$Ge_2Sb_2Te_5$ films, following the idea that the phenomenon could be induced by avalanche breakdown [34-37].

4. Critique

The lucky-drift model, though having given more accurate descriptions of the avalanche breakdown in crystalline semiconductors [8,28-31], may lead the understanding of the phenomenon in disordered semiconductors to tangled labyrinths, with the following reasons:

First, the concept of phonons in disordered semiconductors should be carefully employed [56,57]. Since there exists no long-range atomic periodicity in amorphous structures, neither the phonon wavenumber nor the dispersion relation can be fixed. In addition, to separate out acoustic and optical phonons, it is prerequisite to define a periodically-arranged unit cell containing more than one atom, which is clearly impossible for the disordered structure in a-Se, illustrated in Fig. 3(a). We can just evaluate, using neutron and Raman scattering experiments, the vibrational density-of-state, which may be resolved in to long-wavelength sound waves, molecular vibrations, and unspecified vibrations giving rise to a Boson peak.

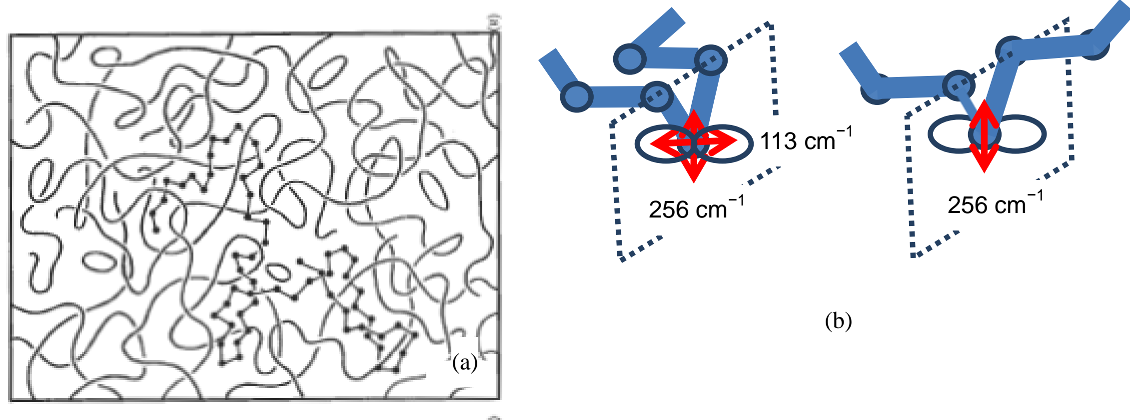

Fig. 3. (a) An entangled chain structure of a-Se [6], and (b) atomic vibrations of (left) cis and (right) trans conformations [44,57] with lone-pair wave-functions being drawn only for the vibrating atoms.

Second, carrier transport in disordered semiconductors, specifically at high fields, remains to be studied. How can we analyze the interaction of warm or hot holes (and electrons) with vibrational and static structural disorders? It has been demonstrated that carrier transport at low fields is suppressed with *trapping* by localized states, while *scattering* has hardly been analyzed [35,56], and the distinction between these two processes through experiments and theories seems to be difficult for disordered semiconductors. For instance, the known temperature dependence $\mu \sim T^{-3/2}$ [8] arising from scattering of carriers with acoustic phonons has never been demonstrated in amorphous semiconductors. In addition, a-Se (and also c-Se) is a lone-pair semiconductor, in which the conduction and the valence band have different characters, being composed with anti-bonding and lone-pair states [6,56], and accordingly, electron- and hole-lattice interactions must appreciably be different [53]. We should also consider plausible formation of *polarons* in flexible chain structures [16,41,58]. At high fields, however, we may envisage that the carrier transport in amorphous semiconductors becomes more-or-less free. For instance, the Poole-Frenkel mechanism [36] provides, at F = 1 MV/cm and ε_r = 10, lowering of Coulombic barriers by 0.2 eV at a distance of 1 nm where the barrier is maximal. Under such conditions, can we neglect the trapping process, taking only the scattering with disordered potentials into account?

Third, the modified lucky-drift model predicts very short mean free paths between elastic collisions, e.g., ~0.4 nm for holes (Table 1). The length is comparable to the atomic distance of 0.24 nm [44], which casts doubt upon the particle picture of the model. Otherwise, a random-phase model [35,56] assumes quantal behaviors of electrons in amorphous semiconductors under high fields, while we wonder if the phase of electron wave-functions could be defined for such a short path length. Note that, in crystalline semiconductors, the lucky-drift model provides much longer (>> a) paths, e.g., $L_{elastic}$ = 8 and 5 nm for electrons in Si and GaAs [8,30].

Finally, although the modified lucky-drift model has been refined, detailed, and simulated, there still remain

substantial deviations of calculated $\gamma(F)$ curves from the experimental results, as exemplified in Fig. 2 [25]. In addition, the model has been unable to suggest the origin of the temperature dependence, $\partial\gamma/\partial T > 0$ [25].

5. Proposals

At the outset, we briefly summarize atomic structures and related properties of a-Se. As illustrated in Fig. 3(a), pure a-Se (which may be stabilized at ~50 °C) is assumed to be composed mainly of entangled Se chains, with a few ring molecules, the content depending upon preparation procedures [44,57]. The number of atoms in single chains is estimated at ~10^5 [6,44], so that the density of chain ends (dangling bonds) is $10^{17} - 10^{18}$ cm^{-3}, which may be ionized (C_1^-) or neutral (C_1^0). Nevertheless, the density of such defects (including C_3^+ and C_3^0) seems to be too small to govern carrier transport. It has also been known that oxygen causes a decisive impurity effect on the electrical conductivity in a-Se [6,44], while its extent at high fields has not been known. (The purity of a-Se films has not been specified in previous studies, except that As may be doped for stabilization [5].) On the other hand, it is un-doubtful that the chain consists of cis- (turned) and trans-like (helical) structures, as shown in Fig. 3(b), which become the sources producing acoustical and molecular vibrations. For the former, using the longitudinal sound velocity V_s (~1.8×10^5 cm/s [59]) and assuming a vibrational wavelength of ~$5a$ ($a = 0.24$ nm), which may represent the length of segmental chains, we obtain a vibrational energy $\hbar\Omega$ of ~5 meV. For the molecular vibration, theoretical analyses [44,57] have reproduced the experimentally observed two modes illustrated in Fig. 3(b); stretching (~30 meV, ~256 cm^{-1}) and bending (~14 meV, ~113 cm^{-1}), in which the latter probably exerts stronger effects upon hole transport, since the bending mode has greater vibrational amplitudes (reflecting smaller force constant), giving rise to greater modifications of the lone-pair states.

We also underline that Tsuji et al. [14] have approximated their $\gamma(F)$ result with two exponential curves, as shown in Fig. 2, at moderate (0.8–1.3 MV/cm) and high fields (1.3–1.6 MV/cm). The equations given by them [14] can be converted, using Eq. (1), to the parameters listed in Table 1, in which the E_i values suggest two excitation processes; sub-gap and band-to-band impact ionizations. (Naturally, the obtained moderate-field parameters are similar to those by Arkhipov and Kasap [20].) Note that the high-field behavior, which is difficult to inspect using thick films, has not been attained in later experiments (Fig. 2) and that such a two-fields fitting has been dismissed in recent analyses (Table 1). We here proceed following the Tsujis' result.

Under the moderate filed, as illustrated in Fig. 4(a), a photogenerated and field-accelerated hole initiates a sub-gap ionization process. Holes are still "warm" with kinetic energies of a few 10 meV (~k_BT), which are insufficient to excite band-to-band ionization. Nevertheless, the warm hole can impact a band-edge state above the valence band, probably a Urbach-edge state [6,60], which will be ionized negatively after generating a hole. However, the multiplication factor of only ~10 (Fig. 1(a)) under the filed [13-18] implies that, provided the illumination is not intense, the density of ionized sites remains much less than the density of the edge state, ~10^{20} cm^{-3} [6,56,60]. On the other hand, in this situation, as shown in Fig. 1(a), electrons can hardly participate to the breakdown, since electrons are less mobile ($\mu \leq 0.05$ cm^2/Vs [2,3,15]), and in addition, no enough states are assumed to exist below the conduction band [6,60]. It should be mentioned here that such a unipolar avalanche process is favored for low-noise operations of photo-detectors [8].

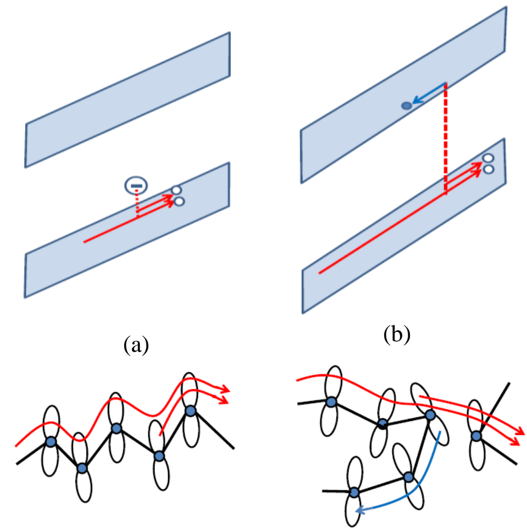

Fig. 4. Band models (upper) and structural illustrations (lower) of (a) sub-gap hole excitation under a moderate field and (b) band-to-band impact ionization under a high field, both being induced by a photogenerated hole.

The sub-gap process, illustrated in Fig. 4(a), resembles impurity impact-ionization in doped semiconductor crystals [31,61,62]. Neutral impurities in the crystal behave herein as impacted Se atoms. We may then estimate the threshold field F_t using an equation derived from an impurity-ionization model [61];

$$F_t \approx (2V_s/\mu)\{(\delta E_e/2k_BT) - 1\}^{1/2}, \qquad (2)$$

where V_s is the longitudinal sound velocity (~1.8×10^5 cm/s [59]), μ the (microscopic) mobility (~1 cm^2/Vs for holes at 300K [2,3]), δ (≤ 1) a constant reflecting energy distribution of accelerated carriers, and E_e represents the energy depth of impacted states. In this equation, –1 denotes the energy gain from atomic vibrations. Assuming $\delta = 1$ and $E_e = 100$ meV, which corresponds to the depth of Urbach-edge states [6,60], we obtain $F_t \approx 0.4$ MV/cm at 300K, which increases to ~0.8 MV/cm at 100K if the other parameters are fixed.

These $F_t(T)$ values are, despite of the simple form of Eq. (2) and rough estimations of the parameters, consistent with the observations in Fig. 1(b) [14].

The threshold field has been predicted also by Mott [36], assuming an energy gain-dissipation balance for an accelerated-and-scattered carrier, as;

$$e\mu F_t^2 \approx \hbar\Omega^2, \quad (3)$$

where $\hbar\Omega$ is a vibrational energy. Note that this equation is independent of T and the electronic energy, E_e or E_i. Assuming $\mu \approx 1$ cm^2/Vs and $\hbar\Omega \approx 30$ meV, we obtain $F_t \approx 1$ MV/cm, which is also comparable with the observations.

Under the high field, a hole becomes hot, and now is able to induce band-to-band impact ionization, producing a secondary hole and also an electron, as illustrated in Fig. 4(b). To delineate the essence, we here use Eq. (1) with Tsujis' high-field formula (Eq. (2') in [14]), obtaining (Table 1) $E_i = 1.9$ eV, which is similar to the optical gap, and $L = 2.6$ nm (~10a), which appears to be a plausible value in comparison with those, 10 − 30 nm [29-31], in crystalline semiconductors.

Putting $\gamma(F_t) = 1/d$ in Eq. (1), we also obtain;

$$F_t = E_i/\{eL \ln(d/L)\}, \quad (4)$$

in agreement with the decreasing F_t with increasing d [14]. Quantitatively, the equation gives, with the parameters given above, $F_t \approx 1.4 \sim 1.0$ MV/cm for $d = 0.5 \sim 4$ μm, which reproduces the observations [14]. (We here bypass discussion for electrons, since the data have been limited [2,3,14] and the expression in [14] gives unreasonably small L values [19], which may be affected by avalanching holes).

For the positive temperature dependence of γ, we can envisage, at least, three possible factors. One is effects of geminate recombination, which have been considered previously [13,19,25]. The other may arise from a change in transport mechanisms, from dispersive to Gaussian [6,56,63], while the effect on $\gamma(T)$ is difficult to evaluate. The last is a vibrational effect on the bandgap energy, which can be taken into account by assuming $E_i \approx E_g$, the latter in a-Se under zero fields being demonstrated to follow the Fan's one-oscillator type temperature variation;

$$E_g(T) = E_g(0) - An(T), \quad (5)$$

where $n(T) = \{\exp(E_R/k_BT) - 1\}^{-1}$, with a fitting parameter A of 0.26 eV and $E_R = 24$ meV [64]. (E_R is naturally in between the vibrational energies of ~14 and ~30 meV.) Inserting Eq. (5) and $E_g(0) = 2$ eV into Eq. (1) with a tentative assumption of fixed L (= 2.6 nm), we obtain $\gamma(300\text{K}) = 2.1 \times 10^4$ cm^{-1} and $\gamma(150\text{K}) = 1.6 \times 10^4$ cm^{-1} at $F = 1.4$ MV/cm, which are comparable with the Tsujis' results [14], ~2.0×10^4 and ~0.9×10^4 cm^{-1}. Note that the present idea, Eq. (5), is equivalent to assume that drifting carriers *gain* thermal energy through electron-lattice interaction, in a similar way to the phonon *absorption* in crystalline semiconductors. Such a thermal activation effect possibly becomes more prominent in the sub-gap process, since the depth of the Urbach edge is only ~100 meV (<< 2 eV).

6. Other amorphous films

Steep current increases at high fields, or phenomena resembling the avalanche breakdown, have been reported also in other disordered solids including a-Si:H [32,33], Te-compounds [34-39], and organic films [40-43]. The sample structure and threshold field are, for instance;
an Au/a-SiC:H/a-Si:H(360 nm thick)/c-Si pin diode and ~1.3 MV/cm [33],
metal-sandwiched a-$Ge_2Sb_2Te_5$ films (50 nm thick) and ~0.5 MV/cm [38], and
a perylene pigment film (500 nm thick) sandwiched in between thin Au films and ~0.1 MV/cm [40].

Having seen these structures and threshold fields, we see marked uniqueness of the a-Se samples. One is that the breakdown in a-Se occurs in samples having non-injecting contacts (Table 1), the situation being in contrast to those in all the other films, which are contacted in between metallic electrodes. We also note that the electrical switching (and successive thermal phase changes) in a-$Ge_2Sb_2Te_5$, which is not photoconductive [65], occurs in the dark. Incidentally, the switching phenomenon tends to possess filamentary electrical conduction [34-39], but such a feature has never appeared in the a-Se breakdown. The other is that employed a-Se films are relatively thick (0.5 − 200 μm), in comparison with the others (≤ 0.5 μm), in which growing carrier multiplication may be difficult to occur.

We should consider the mechanisms of the current increases in these non-chalcogen films from two respects:

One is whether the observed current increase is really an avalanche breakdown or not. As mentioned above, those current increases have appeared in samples having metallic electrodes, so that phenomena as carrier injection and/or tunneling (Zener) breakdown can participate, the idea having being suggested for organic films [40,41]. For the electrical switching phenomenon, it may be triggered by the avalanche breakdown ($E_R \approx 20$ meV [23] and $\mu \approx 10^{-3} \sim 10^{-2}$ cm^2/Vs at low fields [66,67]), while a role of (double) carrier injection seems to be a primary factor [36,37], specifically in very thin films of ~50 nm [38]. In anyway, before considering the details, we should examine if the electrical switching occurs in samples having non-injecting electrodes, which is still lacking, to the author's knowledge. (We know that a variety of fundamental properties had been investigated for non-stoichiometric tellurides in 70s [34,37], while those for a-$Ge_2Sb_2Te_5$ remain insufficient).

The other is that the present model predicts that the avalanche breakdown in a-Si:H films can appear only at high fields, which may be in harmony with the observations [33]. Sub-gap ionization under moderate fields is difficult to occur, since in a-Si:H an electron is more mobile than a

hole but the conduction band has fewer excitable edge states than those above the valence band [8]. The higher vibrational energy (80 − 250 meV) of a-Si:H than that in a-Se may also be responsible for the higher breakdown field [15], but such an idea is incompatible with the current increase in organic materials having much higher vibrational and bandgap energies [8].

Finally, we can envisage the occurrence of avalanche breakdowns in other amorphous materials. It seems interesting to investigate high-field behaviors of a-Ge:H, a-Se/Te, and a-$As_2Se(Te)_3$, which have low vibrational energies (~20 meV) with moderate mobility values (< 10^{-2} cm^2/Vs at low fields). Also, it is tempting to examine avalanche breakdowns in a-Se films having co-planar electrodes and liquid Se. In respect of applications, we may obtain higher multiplication factors using bi-layer structures such as a-As_2Se_3/a-Se [68] and polymer/a-Se [69], in which the respective layers can work for photo-carrier generation and avalanching transport. Multi-layer systems have also been demonstrated to be promising [11,70].

7. Summaries

After overviewing and criticizing notable studies on the avalanche breakdown in a-Se, we have proposed a new, simple idea for the mechanism. It straightforwardly takes two kinds of ionization processes, sub-gap and band-to-band, into account, which are analyzed using simple equations. The obtained result, including temperature dependence, can afford plausible explanations for the experimental observations. We have also given some comments on steep high-field current rises and possible occurrence of the avalanche breakdown in other materials.

Acknowledgements

The author would like to thank K. Shimakawa for critical reading and valuable comments, T. Wagner for Czech translation, and K. Tanioka and K. Tsuji for informative private communications.

References

[1] F. Seitz, Phys. Rev. **76,** 1376 (1949).
[2] G. Juška, K. Arlauskas, Phys. Stat. Sol. A **59,** 389 (1980).
[3] G. Juška, K. Arlauskas, Phys. Stat. Sol. A **77,** 387 (1983).
[4] K. Tanikoka, J. Yamazaki, K. Shidara, K. Taketoshi, T. Kawamura, S. Isioka, Y. Takasaki, IEEE Electron Devices Lett. **EDL-8,** 392 (1987).
[5] K. Shirada, K. Tanioka, T. Hirai, Optoelectronics **6,** 311 (1991).
[6] K. Tanaka, K. Shimakawa, Amorphous Chalcogenide Semiconductors and Related Materials (Springer, New York, 2011)
[7] M. Nanba, Y. Takiguchi, Y. Honda, Y. Hirano, T. Watabe, N. Egami, K. Miya, K. Nakamura, M. Taniguchi, S. Itoh, A. Kobayashi, J. Vacuum Sci. Technol. B **28,** 96 (2010).
[8] S. Kasap, P. Capper (eds.), Handbook of Electronic and Photonic Materials (Springer, New York, 2006).
[9] T. Miyoshi, N. Igarashi, N. Matsugaki, Y. Yamada, K. Hirano, K. Hyodo, K. Tanioka, N. Egami, M. Namba, M. Kubota, T. Kawai, S. Wakatsuki, J. Synchrotron Rad. **15,** 281 (2008).
[10] A. Sultana, M.M. Wronski, K.S. Karim, J.A. Rowlands, IEEE Sensors J. **10,** 347 (2010).
[11] M. Z. Kabir, Safayat-Al Imam, Appl. Phys. Lett. **102,** 153515 (2013).
[12] T. Masuzawa, S. Kuniyoshi, M. Onishi, R. Kato, I. Saito, T. Yamada, A. T. T. Koh, D. H. C. Chua, T. Shimosawa, K. Okano, Appl. Phys. Lett. **102,** 073506 (2013).
[13] K. Tsuji, Y. Takasaki, T. Hirai, K. Taketoshi, J. Non-Cryst. Solids **114,** 94 (1989).
[14] K. Tsuji, Y. Takasaki, T. Hirai, J. Yamazaki, K. Tanioka, Optoelectronics **9,** 267 (1994).
[15] A. Reznik, S.D. Baranovskii, O. Rubel, G. Juska, S.O. Kasap, Y. Ohkawa, K. Tanioka, J.A. Rowland, J. Appl. Phys. **102,** 053711 (2007).
[16] A. Reznik, S.D. Baranovskii, O. Rubel, K. Jandieri, S.O. Kasap, Y. Ohkawa, M. Kubota, K. Tanioka, J.A. Rowland, J. Non-Cryst. Solids **354,** 2691 (2008).
[17] O. Bubon, G. DeCrescenzo, W. Zhao, Y. Ohkawa, K. Miyakawa, T. Matsubara, K. Kikuchi, K. Tanioka, M. Kubota, J. A. Rowlands, A. Reznik, Curr. Appl. Phys. **12,** 983 (2012).
[18] A. Reznik, K. Jandieri, F. Gebhard, S.D. Baranovskii, Appl. Phys. Lett. **100,** 132101 (2012).
[19] V. I. Arkhipov, S. O. Kasap, J. Non-Cryst. Solids **266-269,** 959 (2000).
[20] O. Rubel, S. D. Baranovskii, I. P. Zvyagin, P. Thomas, S. O. Kasap, Phys. Stat. Sol. C **1,** 1186 (2004).
[21] S. Kasap, J. A. Rowlands, S. D. Baranovskii, K. Tanioka, J. Appl. Phys. **96,** 2037 (2004).
[22] K. Jandieri, O. Rubel, S.D. Baranovskii, A. Reznik, J. A. Rowlands, S. O. Kasap, J. Non-Cryst. Solids **354,** 2657 (2008).
[23] K. Jandieri, O. Rubel, S. D. Baranovskii, A. Reznik, J. A. Rowlands, S. O. Kasap, Phys. Stat. Sol. C **5,** 796 (2008).
[24] K. Jandieri, O. Rubel, S. D. Baranovskii, A. Reznik, J. A. Rowlands, S. O. Kasap, J. Mater. Sci: Mater Electron **20,** S221 (2009).
[25] O. Rubel, A. Potvin, D. Laughton, J. Phys.: Condens. Matter .**23**, 055802 (2011).
[26] W. Shockley, Solid-State Electron. **2,** 35 (1961).
[27] G. A. Baraff, Phys. Rev. **128,** 2507 (1962).
[28] B. K. Ridley, J. Phys. C: Solid State Phys. **16,** 3373 (1983).

[29] S. McKenzie, M. G. Burt, J. Phys. C: Solid State Phys. **19,** 1959 (1986).
[30] J. S. Marsland, Solid-State Electron. **30,** 125 (1987)
[31] E. Bringuier, Phys. Rev. B **49,** 7974 (1994).
[32] S. Jwo, M. Wu, Y. Fang, Y. Chen, J. Hong, C. Chang, IEEE Trans. Electron Devices **35,** 1279 (1988).
[33] M. Akiyama, M. Hanada, K. Sawada, M. Ishida, Jpn. J. Appl. Phys. **42,** 2345 (2003).
[34] S. R. Ovshinsky, Phys. Rev. Lett. **21,** 1450 (1968).
[35] N. K. Hindley, J. Non-Cryst. Solids **5,** 31 (1970).
[36] N. F. Mott, Philos. Mag. **24,** 911 (1971).
[37] S. Hudgens, Phys. Stat. Sol. B **249,** 1951 (2012).
[38] Y. Yin, S. Hosaka, Appl. Phys. Lett. **100,** 253503 (2012).
[39] A. Cappelli, E. Piccinini, F. Xiong, A. Behnam, R. Brunetti, M. Rudan, E. Pop, C. Jacoboni, Appl. Phys. Lett. **103,** 083503 (2013).
[40] M. Hiramoto, T. Imahigashi, M. Yokoyama, Appl. Phys. Lett. **64,** 187 (1994).
[41] E. M. Conwell, Phys. Rev. B **57,** R12670 (1998).
[42] E. S. Chen, S. H. Yeh, H. F. Meng, Phys. Rev. B **65,** 235206 (2002).
[43] J. Reynaert, V. I. Arkhipov, P. Heremans, J. Poortmans, Adv. Funct. Mater. **16,** 784 (2006).
[44] R. A. Zingaro, W. C. Cooper (eds.), Selenium (Van Nostrand Reinhold Company, New York, 1974).
[45] S. D. Ganichev, J. Diener, W. Prettl, Appl. Phys. Lett. **64,** 1977 (1994).
[46] V. A. Vasil'ev, M. E. Kumekov, M. A. Tagirdzanov, E. I. Terukov, Semicond. **28,** 1172 (1994).
[47] M. Glicksman, M. C. Steele, Phys. Rev. Lett. **2,** 461 (1959).
[48] A. G. Chynoweth, K. G. McKay, Phys. Rev. **106,** 418 (1957).
[49] J. Mort, Phys. Rev. Lett. **18,** 540 (1967).
[50] J. Kodeš, Czech. J. Phys. **16,** 277 (1966).
[51] B. Y. Zhang, C. Yang, W. F. Liu, A. M. Liu, Appl. Phys. Lett. **101,** 093903 (2012).
[52] P. A. Wolff, Phys. Rev. **95,** 1415 (1954).
[53] O. Rubel, D. Laughton, J. Phys.: Condens. Matter **22,** 355803 (2010).
[54] A. Darbandi, O. Rubel, J. Non-Cryst. Solids **358,** 2434 (2012).
[55] A. Darbandi, O. Rubel, Can. J. Phys. **91,** 483 (2013).
[56] S. R. Elliott, Physics of Amorphous Materials, 2nd Ed. (Longman, Essex, 1990).
[57] K. Nakamura, A. Ikawa, Phys. Rev. B **67,** 104203 (2003).
[58] D. Emin, Phys. Rev. B **74,** 035206 (2006).
[59] S. Fukuda, T. Shiosaki, A. Kawabata, Jpn. J. Appl. Phys. 19, 2075 (1980).
[60] K. Tanaka, J. Optoelectron. Adv. Mater. **3,** 189 (2001).
[61] N. Sclar, E. Burstein, J. Phys. Chem. Solids **2,** 1 (1957).
[62] V. Mortet, A. Soltani, Appl. Phys. Lett. **99,** 202105 (2011).
[63] G. Pfister , Phys. Rev. Lett. **36,** 271 (1976).
[64] L. Tichý, H. Tichá, P. Nagels, E. Sleeckx, R. Callaerts, Mater. Lett. **26,** 279 (1996).
[65] K. Tanaka, J. Appl. Phys. **101,** 026111 (2007).
[66] T. Kato, K. Tanaka, Jpn. J. Appl. Phys. **44,** 7340 (2005).
[67] S. A. Baily, D. Emin, H. Li, Solid State Commun. **139,** 161 (2006).
[68] T. Kitamura, S. Imamura, T. Minato, N. Nakamura, J. Non-Cryst. Solids **77-8,** 1249 (1985).
[69] I. H. Campbell, Appl. Phys. Lett. **99,** 063303 (2011).
[70] E. Maruyama, Jpn. J. Appl. Phys. **21,** 213 (1982).

*Corresponding author: keiji@eng.hokudai.ac.jp